Swelling and thermal behavior of a cross-linked polymer networks poly(2-phenoxyethyl acrylate): exploitation by the Voigt viscoelastic model

Nouara Benmessaoud, Salah Hamri, Tewfik Bouchaour, Ulrich Maschke

Swelling and thermal behavior of a cross-linked polymer networks poly (2-phenoxyethyl acrylate): exploitation by the Voigt viscoelastic model

Nouara Benmessaoud[1] Salah Hamri[1,2]· Tewfik Bouchaour[1]

Ulrich Maschke[3]

Abstract

The response-ability to the external and internal environmental condition qualifies the smart polymer material to be successfully applied in artificial muscle, drug delivery and water treatment. A three-dimensional polymer network based on the phenyl monomer, 2-phenoxy ethyl acrylate (PEA), was polymerized under ultraviolet (UV) radiation using the Darocur 1173 as an initiator of the polymerization reaction, and the 1,6-hexane-diol diacrylate (HDDA) as a chemical cross-linker. The analysis of the thermophysical properties of this elaborated polymeric material represents the main goal of the present work. The infrared spectroscopy (FTIR) and the dynamic scaling calorimetry (DSC) were used to examine,

respectively, the vibration of the carbon double bond (C=C) and the glass transition temperature T_g. It is found that parameters, the rate of reticulation and monomer composition have a remarkable effect on the variation of T_g. The swelling behavior of the cross-linked poly(PEA/ HDDA) was investigated; the effects of solvent nature, the degree of cross-linking, temperature and chemical structure have a significant influence on material swelling properties. The theoretical investigation based, especially on the Voigt model, Flory–Rehner theory and solubility approximation, permits to give much information about several parameters such as the swelling time constant, swelling equilibrium constant, solubility prediction, entropy and enthalpy. It ended interestingly that the Voigt model shows a good agreement with swelling experimental results.

Keywords Cross-linked network · UV photopolymerization · Glass transition temperature · Swelling · Voigt model

Introduction

Intelligent material has a smart behavior toward the internal and external conditions such as temperature [1], pH of the medium [2], magnetic and electric field [3, 4]. The investigation of the intelligent comportment of such material was the principle motivation for many researchers and encourages them to invent mechanisms, techniques, experimental and theoretical tools [5, 6].

Among the experimental method, the swelling study permits to analyze the physical properties of substances [7, 8]. Material with swelling capacity can be used in numerous applications; in drug delivery, the polymer networks can be used to release a medicament after swelling in the stomach; pH in this application was considered as a stimulus [9]. In the oil and gas sector, swelling elastomers have been successfully deployed in zonal isolation where it is used to separate between unwanted and production zones, and this permits to avoid the mixing of redundant fluids. Furthermore, it can be applied to be a partial replacement of cement and to slim the down of wells [10]. It helps also to improve the volume of production and the recovery rate of hydrocarbons, thus reducing the impact on the environment. Additionally, the swelling polymer has been widely used for the cleanup of the water surface from organic solvents and

petroleum waste [11–13].

The phenomenon of swelling of polymer networks is a classical subject of polymer science. Many years ago, Flory and Rehner [14] developed a theory of rubber elasticity, suggesting that the swelling equilibrium is reached when the osmotic pressure of small solvent molecules that promote swelling is balanced by the elastic forces at the cross-links opposing network strand extension. In 1978, Tanaka [15] discovered that polymer gels change volume discontinuously and reversibly in response to external environmental changes such as pH, temperature and solvent composition. Since the discovery of this phenomenon, the study of polymer gels has progressed rapidly. Recently, Kowalski et al. [16] studied the effect of the structure on the swelling properties of poly(acrylic acid) high methylated pectin hydrogels which are obtained by free radical polymerization/grafting reaction. It was found that the introduction of a small amount of pectin to the hydrogel increases the swelling capacity, but the further increase in pectin content causes a deterioration of these properties.

Idaat et al. [17] evaluated the effect of monomer sequence along the network chain of polymer gels on the swelling behavior by utilizing two gel synthetic methods, copolymerization and co-cross-linking. It was found that the swelling measurement of the obtained gels showed

totally different behaviors between the copolymerization and the co-cross-linking gels.

Bendahma et al. [18] presented a study about the removal of eosin Y from water; the three-dimensional poly(2-hydroxyethyl methacrylate)- designed poly(HEMA) was used as retention support. Uptake of water by swelling of hydrogel permits to the pollutant, eosin Y, to be well retained by the porous polymer network poly(HEMA).

In the present work, the polymer network based on an aromatic acrylic monomer was elaborated by the UV light curing technique with many advantages such as the carries out at room temperature, no solvent required and time reduction. The difunctional monomer HDDA was used to cross-link the polymer chains which product a three-dimensional architecture of the elaborated polymer.

To our knowledge of the literature, there is no study of the swelling and determination of thermophysical properties peculiarly for the polymer networks poly(2-phenoxy ethyl acrylate)-designed poly(PEA). The monomer 2-phenoxy ethyl acrylate was chosen for several reasons: (a) the presence of the aromatic ring in its chemical structure ensures thermal stability which makes it possible to obtain a thermally stable polymer material. (b) The structure of this monomer also makes it

possible to obtain flexible materials unlike other aromatic polymers such as polystyrene which has a rigid structure. (c) The presence of the acrylate function, very reactive, allows a good conversion rate by photopolymerization under UV radiation.

Polymer architecture was varied by two parameters, the degree of reticulation and the degree of copolymerization; the first parameter was increased by the increase in the HDDA cross-linker quantity, whereas the copolymerization was realized by the introduction of another monomer, named lauryl acrylate noted LA, as results, these parameters affected clearly the glass transition temperature T_g.

The kinetics of swelling of the poly(PEA) was investigated to examine the effect of solvent nature, two isotropic solvents, polar aliphatic and apolar aromatic, respectively, and toluene and MIBK were chosen to swell the polymer networks. It is found that toluene is a good solvent, whereas the MIBK is a bad solvent; this results due to the different chemical structures of solvents. Porosity was varied by the increase in the percentage of the difunctional monomer HDDA, consequently, a decrease in swelling in toluene and MIBK is noted, respectively, from 130 to 55% and from 68 to 30%. Chemical structure factor was varied by the introduction of the monomer LA that has a long linear chemical structure; it noted an increase in the swelling rate due to the basic

chemical structure. The temperature was also varied; the phase diagram shows different behaviors in the case of the two previous solvents.

On the other hand, the Voigt viscoelastic model consists of applying stress, in parallel, on an elastic spring and a viscous damper, which associated, respectively, to the two resistances of the network expansion and molecule diffusion. This model is considered as the best known and the most often applied to model the creep and relaxation behavior of polymer, especially in the study of hydrogels [19–21]. It is successfully applied in the present work, for the swelling study of poly(PEA) networks in organic solvents.

The Voigt viscoelastic model allows for analyzing the present swelling results. In fact, theoretical parameters, the time swelling constant explain the diffusion of toluene/MIBK solvents and the equilibrium constant explains the plate obtained, many equations were proposed to explain the present experimental results, and it noted the good correlation between experimental and theoretical results.

Experimental part

Materials

The acrylic monomer used in this study is 2-phenoxy ethyl acrylate (PEA) that was provided, by Sigma-Aldrich. Lauryl acrylate (LA)

(from RAHN AG). The cross- linking agent is 1,6-hexane-diol diacrylate (HDDA) (obtained from Cray Valley, France). The photopolymerization agent used is 2-hydroxy-2-methyl-1-phenyl-propane-1 (Darocur 1173, from Ciba Geigy). The chemical structures of the different components are shown in Fig. 1. The two solvents used in this study are toluene and methyl isobutyl ketone MIBK purchased from Sigma-Aldrich.

Sample preparation and FTIR examination

The elaboration of polymer networks was made by irradiating the mixtures of three basic components (monomer, cross-linker and photoinitiator) using a UV lamp (Philips TL08 type with a wavelength characteristic, λ = 365 nm and intensity of I_0 = 1.5 mW/cm^2) in an inert atmosphere, created by a stream of nitrogen gas cir- culating in a quartz chamber that contains the sample holder (a cylindrical Teflon mold).

Fourier transform infrared FTIR spectra were recorded in the range of 4000–600 cm^{-1} with PerkinElmer Frontier FTIR model spectrometer, in ATR mode, with a spectral resolution of 4 cm^{-1}. The number of scans accumulated was 16.

The reagent solution was examined by FTIR, before and after

polymerization. 20 min was the time of exposition under UV light, to achieve a quasi-complete conversion of monomers (98%) in the precursor system; however, Fig. 2 shows the quasi-total disappearance of the acrylate characteristic band (C=C) at 1635 cm^{-1}. The cross-linked polymers networks obtained based on poly(PEA) and poly (PEA- co-LA) were flexible and optically transparent.

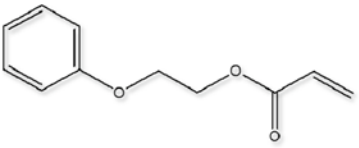

2-phenoxy ethyl acrylate (PEA)

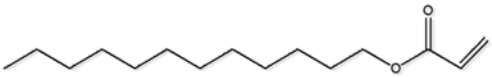

Lauryl acrylate (LA)

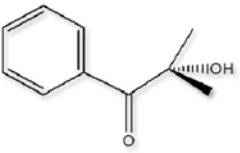

Darocur 1173

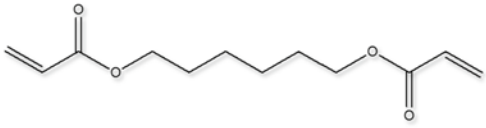

1,6-hexanediol diacrylate (HDDA)

Fig. 1 Chemical structure of the components of the initial mixtures

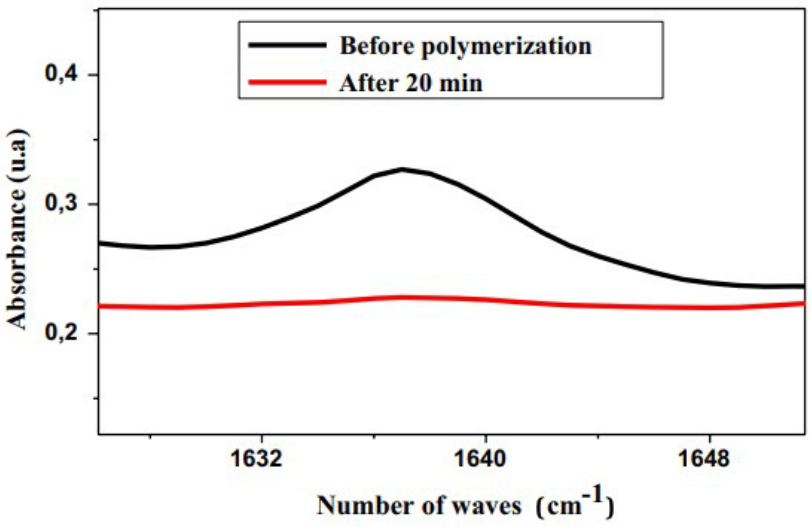

Fig. 2 Illustration of the disappearance of the characteristic band of acrylates (C=C) at 1635 cm^{-1}

Differential scanning calorimetry DSC

The glass transition temperature and heat capacity were determined by differential scanning calorimetry (DSC) using a PerkinElmer Pyris Diamond DSC 8000 apparatus. Samples of about 5 mg were analyzed under nitrogen gas flow at a heating rate of 10 °C/min from −72 to 230 °C.

Swelling measurements

To study the swelling kinetic behavior, a cylindrical sample was weighed and immersed in a different solvent at room temperature. The sample was taken out at regular intervals of time, wiped with a filter paper to remove the free liquid on the surface and then weighted. The degree of swelling is calculated from the following expression 1:

$$\tau\ (\%) = 100.\left(m_t - m_0 / m_0\right) \qquad (1)$$

where τ (%) is the degree of swelling. m_t is the weight of the swollen network at time

t. m_0 is the weight of initially dried network.

Theoretical part

The exploitation of the Voigt viscoelastic model allows analyzing efficiently the swelling kinetics results. The Flory–Rehner model permits to determine the phase diagrams of the polymer/solvent mixture.

The thermodynamic parameters especially, the enthalpy, entropy and free energy, were determined by van't Hoff's equation. The solubility calculation predicts the solubility of polymer networks in the chosen

solvent.

The Voigt model

The Voigt model is based on Eq. 2 which relates between swelling rate and two important parameters, the swelling time constant and the power parameter.

$$Q(t) = Q_{max}\left[1 - \exp\left(\frac{t}{\tau_s}\right)\right] \quad (2)$$

where $Q(t)$ is the rate of swelling at time t. Q_{max} called the power parameter which measures the resistance to the polymer network expansion and the equilibrium degree of swelling. τ_s called the swelling time constant or rate parameter which measures the resistance to solvent diffusion.

Solubility model

It is theoretically possible to predict, approximately the solubility of the polymer in a solvent, as expressed by Eq. 3:

$$S \approx (\delta_p - \delta_s)^2 \quad (3)$$

where δ_p is the solubility parameter of the polymer and δ_s is that of the solvents calculated by the method of Hoftyzer and Van Krevelen (HVK) [22, 23] as it is expressed in Eq. 4. The units for these

parameters are $(MPa)^{1/2}$. The solubility parameter can be expressed according to the three solubility parameter:

$$\delta_t^2 = \delta_d^2 + \delta_p^2 + \delta_h^2 \quad (4)$$

where δ_d, δ_p and δ_h are the Hansen solubility parameters for the dispersion, polar and hydrogen bonding interactions, respectively, which can be estimated from the group contributions using Eqs. 5, 6 and 7:

$$\delta_d = \frac{\sum F_{d_i}}{V} \quad (5)$$

$$\delta_p = \frac{\left(\sum F_{p_i}\right)^{1/2}}{V} \quad (6)$$

$$\delta_h = \left(\frac{\sum E_{h_i}}{V}\right)^{1/2}. \quad (7)$$

F_{d_i} and F_{p_i} are, respectively, the molar attractant constants for the dispersive and polar components. E_h is the cohesion energy that describes the contribution of the hydrogen bond, and this parameter is calculated based on the Small method [24]. V is the molar volume of the unit of material.

Phase diagrams

The phase diagrams provide information on the thermodynamic stability of the coexistence phases as a function of temperature and composite. Experimentally, it can be obtained by plotting temperature versus solvent weight fraction (φ_S) which can be calculated from Eq. 8:

$$\varphi_s = \tau/(\tau + 1) \quad (8)$$

The phase diagrams can be determined by means of the FloryRehner theory.

Flory–Rehner theory

The main hypothesis of this theory is that the change in free energy consists of sepa- rable and additive quantities [25]. These are the free energy of mixing ΔG_{mix} and the free energy of elastic strain ΔG_{el} as expressed in Eq. 9:

$$\Delta G = \Delta H - T\Delta S \quad (9)$$

In order to determine the phase diagram, the chemical potential which can be obtained from the derivative of the free energy. The chemical potentials [26] of solvent and polymer denoted, respectively, μ_s and μ_p, are defined on Eqs. 10 and 11 as follows:

$$\mu_s = \left(\frac{\partial(\Delta G)}{\partial n_s}\right)_{n_p, P, T} \quad (10)$$

$$\mu_p = \left(\frac{\partial(\Delta G)}{\partial n_p}\right)_{n_s, P, T} \quad (11)$$

where P is the pressure, T is the absolute temperature, n_s and n_p are numbers of molecules of solvent and polymers, respectively.

Equations 12 and 13 correspond to the chemical potentials of the solvent and the polymer, respectively, obtained from Eqs. 10 and 11:

$$\mu_S = k_B T n_S \left\{ \frac{\alpha}{N_C} \varphi_0^{2/3} . \varphi_P^{1/3} - \frac{\beta \varphi_P}{N_C} + \frac{\varphi_P \ln \varphi_S}{n_S} + \chi \varphi_P^2 \right\} \quad (12)$$

$$\mu_P = k_B T \left\{ \begin{array}{l} \frac{\alpha}{N_C} \varphi_0^{2/3} . \varphi_P^{1/3} - \frac{\beta \varphi_P}{N_C} + \frac{\varphi_P \ln \varphi_S}{n_S} + \chi \varphi_P^2 + \frac{3\alpha\varphi_0}{2N_C} \left[\frac{\varphi_P^{-2/3}}{3} - 1 \right] \\ + \frac{\beta}{N_C} (1 + \ln \varphi_P) - \frac{1 + \ln \varphi_S}{n_S} + \chi (\varphi_S - \varphi_P) \end{array} \right\} \quad (13)$$

where the elasticity parameters α and β are obtained from Petrovic model, Eq. 14:[27]

$$\alpha = \frac{f - 2 + 2\varphi_p}{f} \quad \text{and} \quad \beta = \frac{2\varphi_p}{f} \quad (14)$$

where α and β represent the network elasticity parameters. f being the functionality of the monomers. k_B is the Boltzmann constant. φ_S and φ_P represent, respectively, the volume fraction of the solvent and the

polymer. N_c represents the average number of repetitive units at two consecutive cross-linking points. φ_0 is the volume fraction of the polymer network in the reference state (dried network). χ is the interaction parameter of Flory–Huggins.

Thermodynamic quantities, ΔH, ΔS, ΔG

In order to calculate the heat of absorption ΔH, the equilibrium absorption constant K_s was calculated from considerations of the equilibrium process occurring in the liquid phase at constant temperature and pressure, as expressed on Eq. 15:

$$K_s = \frac{\text{mass of absorbed solvent}}{\text{mass of dried network polymer}} \quad (15)$$

Thus, by realizing the relations between K_s and various thermodynamic quantities, enthalpy ΔH and entropy ΔS can be calculated using Eq. 16 of van't Hoff [28].

$$\log K_s = \frac{\Delta S}{2.303R} - \frac{\Delta H}{2.303RT} \quad (16)$$

ΔG values were obtained using the expression 17:

$$\Delta G = \Delta H - T\Delta S \quad (17)$$

Results and discussion

Glass transition examination

To examine the glass transition temperature, two parameters will be varied, the degree of cross-linked and the degree of co-monomers.

Influence of the degree of cross-linking

As shown in Fig. 3, the increase in the cross-linker percentage increases the glass transition temperature of a polymer matrix poly(PEA/HDDA). This effect can be explained in terms of the internal mobility of the system. Indeed, the presence of cross-linking points between the polymer chains reduces the overall mobility of the system. Thus, a reduction in the mobility of the molecules leads to an increase in the T_g because it requires more thermal energy to cause the movements of the polymer chains.

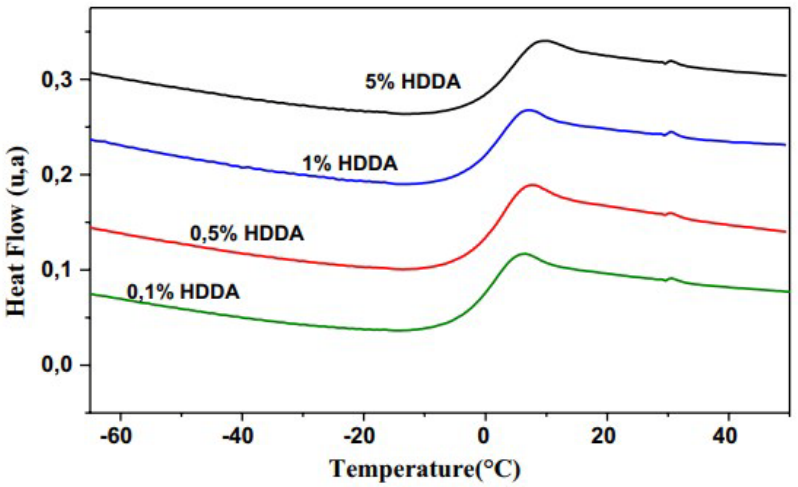

Fig. 3 DSC thermograms of polymer networks poly(PEA/HDDA)

On Fig. 4, the T_g increases as the degree of cross-linking increases and seems to be exponential. On Fig. 5, the evolution of the heat capacity ΔC_p (related to the glass transition) as a function of the degree of cross-linking is presented. It appears that cross-linking has no significant influence on ΔC_p which remains substantially constant.

Influence of the degree of comonomer

Figure 6 represents the DSC thermograms of different copolymer networks (PEA-co-LA/0.1wt% HDDA). The addition of LA

monomer, from 0 to 10%, decreases the glass transition temperature T_g.

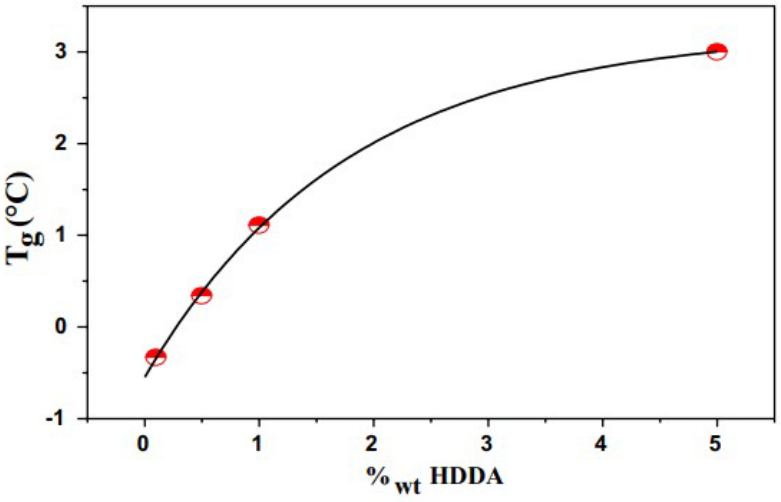

Fig. 4 Glass transition temperature T_g versus (wt% HDDA)

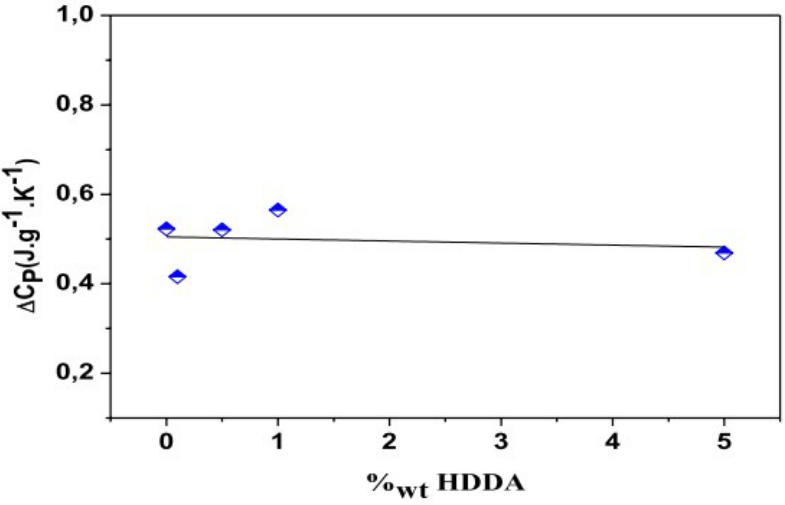

Fig. 5 Heat capacity ΔC_p versus (wt% HDDA)

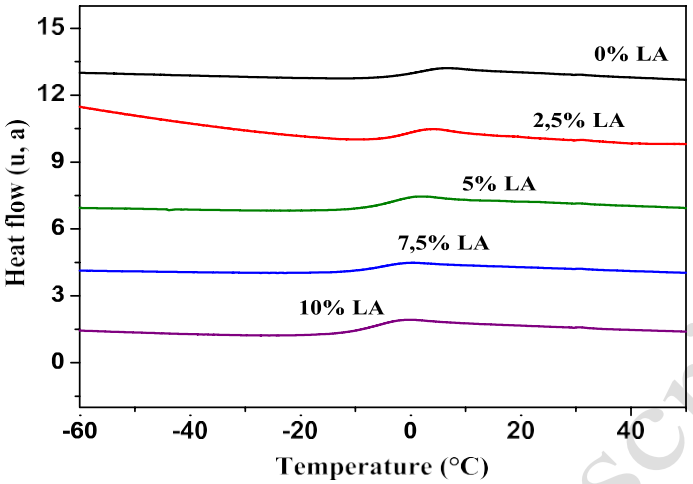

Fig. 6 DSC thermograms of poly(PEA-*co*-LA/0.1wt% HDDA) networks

Figure 7 shows a linear relationship between the glass transition temperature and the degree of lauryl acrylate (wt% LA). The static distribution of these aliphatic monomers, characterized by their long chains, makes the aromatic rings separate and away from those of monomers of PEA, which increases the internal mobility of the system and consequently the decrease in T_g values.

On Fig. 8, the heat capacity decreases slightly as the degree of co-monomer (wt% LA) increases.

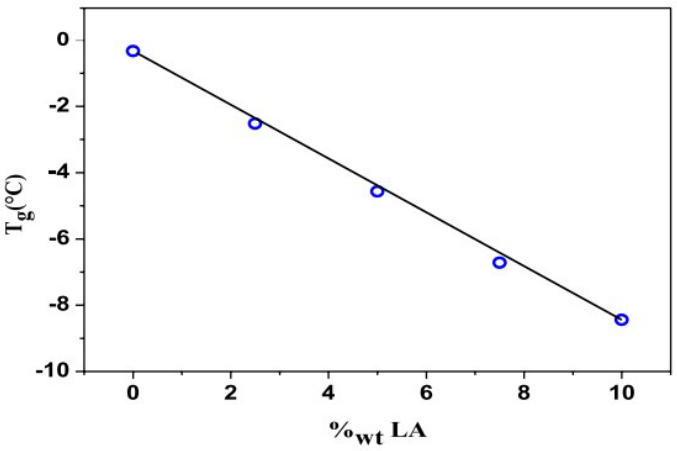

Fig. 7 Glass transition temperature T_g versus (wt% LA)

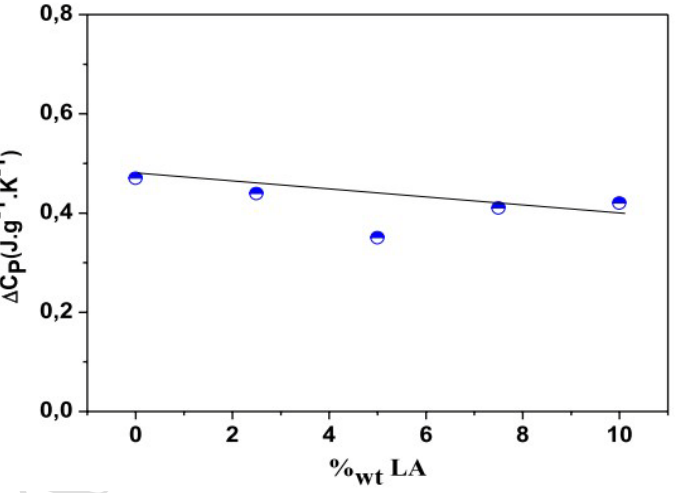

Fig. 8 Heat capacity ΔC_p versus (wt% LA)

Swelling behavior investigation

The effects of the cross-linking agent and copolymerization on the swelling ratio were studied. The swelling time constant and

equilibrium degree of swelling are obtained from Eq. 2.

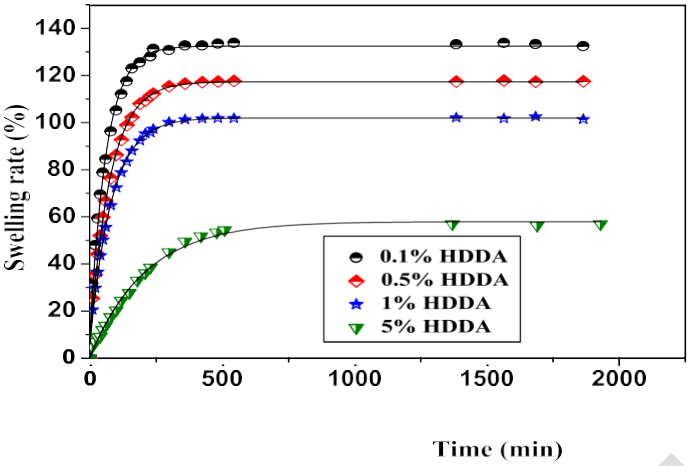

Fig. 9 Kinetics swelling of poly(PEA/HDDA) networks in toluene. Solid curves are the fit to Eq. 2

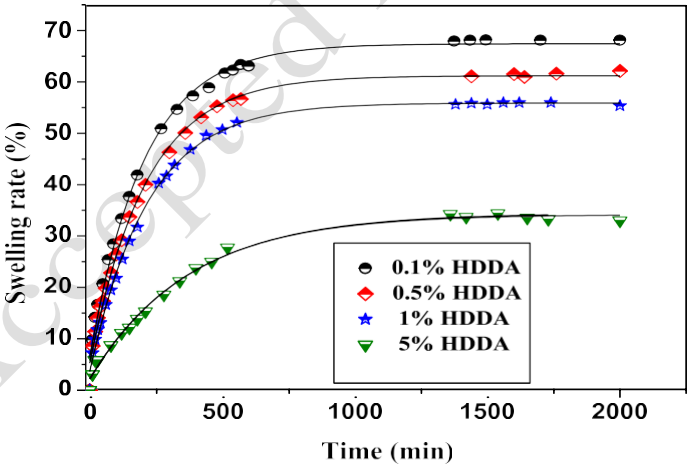

Fig. 10 Kinetics swelling of poly(PEA/HDDA) networks in MIBK. Solid curves are the fit to Eq. 2

Effect of the cross-linking agent

The comparative study of the swelling behavior of poly(PEA/HDDA) in two solvents was presented; it is clear from Figs. 9 and 10 that the polymer network low cross-linked has the largest swelling, nature solvent effect shows a remarkable effect; in fact, the polymer network swells highly in toluene and attained a swelling rate about 130%, whereas in MIBK, the swelling rate is registered at 68%. Solubility approximation can be calculated based on Eq. 3, it concluded from Table 1 that toluene is more miscible with the poly(PEA) network than MIBK, which confirms the experimental results of swelling, for the system poly(PEA/0.1%$_{wt}$ HDDA).

Table1: The solubility of poly(PEA) model networks/ solvents.

Solvent	δ_s (MPa) [23]	S (poly(PEA))
Toluene	18.2	2.69
MIBK	17	8.06

The solubility parameter of poly(PEA/HDDA) was calculated by the VHK method, $\delta_p = 19.84$ MPa

Based on Eq. 2, the experimental data permit to determine the τ_s and Q_{max} values. A good correlation is noted between theoretical and experimental data justified by the value of the coefficient of determination, $R^2 \approx 0.99$ for all curves.

The variation of the swelling time constant τ_s as a function of the degree of cross-linking (wt% HDDA) is shown in Fig. 11. The linear relationship is determined and expressed in Eqs. 18 and 19 which relate between the two previous parameters, for the solvents, toluene and MIBK, respectively:

$$\tau_s = 57.49 + 30.34\ C \qquad (18)$$

$$\tau_s = 194.91 + 35\ C \qquad (19)$$

where C represents the degree of cross-linking of polymer networks ($\%_{wt}$ HDDA).

Figure 12 illustrates a power–law relationship between the equilibrium degree of swelling and degree of cross-linker as you can see on Eq. 20:

$$Q_{max} = a.(1 + C)^b \qquad (20)$$

where a and b are constants for an individual gel, and their values are shown in Table 2.

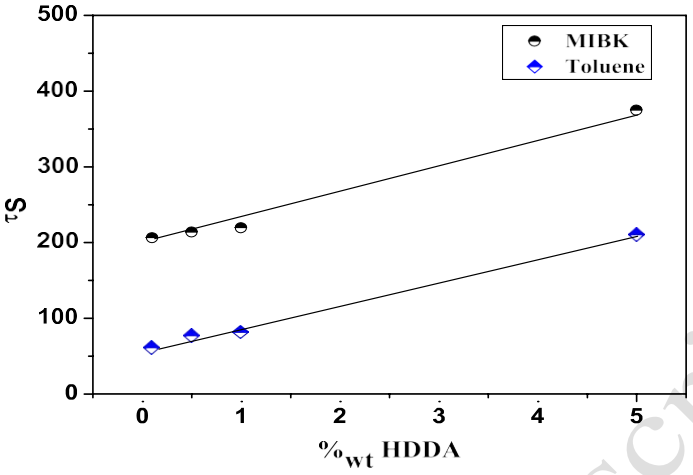

Fig. 11 Swelling time constant (τ_s) versus (wt% HDDA). Lines are guides to the eye

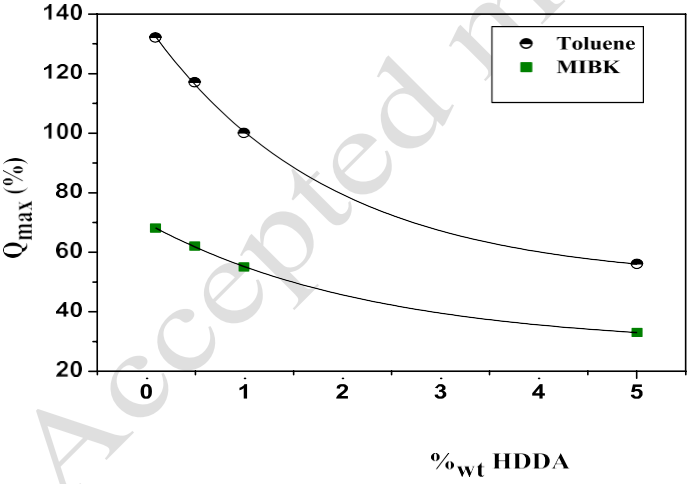

Fig. 12 Equilibrium degree of swelling (Q_{max}) versus (wt% HDDA)

Table 2 : Representation of the values a, b and the coefficient of determination R2 for the two systems

	a	b	R^2
Toluene	140	−0.5008	0.9947
MIBK	72	−0.4207	0.9888

The diffusion of a solvent through a polymer matrix results in the relaxation of the polymer chains previously entangled. Thus, cavities are formed between the cross-linking points allowing mobility and diffusion of the solvent molecules.

However, a highly cross-linked polymer structure will inhibit the transport process more than a low cross-linked polymer network because such chains are more closely bonded together and resist to the increase in the polymer porosity and consequently, increases the diffusion of solvent molecules and the energy required to create such porosity will be important.

Effect of copolymerization

Figures 13 and 14 show the influence of the copolymerization rate on the swelling kinetics. The increase in LA monomer improves the swelling in toluene and MIBK, respectively, from 130 to 200% and

from 68 to 120%. Using Eq. 2, a better fit was obtained to the experimental data.

The variation of the swelling time constant τ_s as a function of the mass ratio of the co-monomer, lauryl acrylate (%wt LA) is illustrated in Fig. 15. The curves have a linear shape with a negative slope. This linear plot can be expressed for two systems poly(PEA)/toluene and poly(PEA)/MIBK, respectively, by Eqs. 21 and 22:

$$\tau_s = 68.37 - 2.54\ C' \qquad (21)$$

$$\tau_s = 173.96 - 7.54\ C' \qquad (22)$$

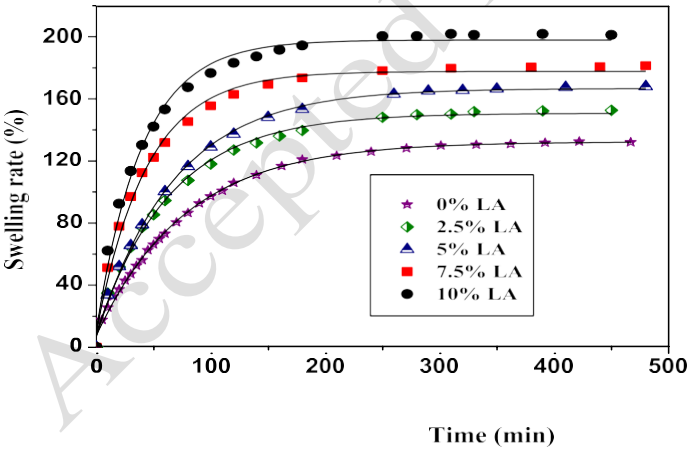

Fig. 13 Kinetics swelling of poly(PEA-*co*-LA/0.1%wt HDDA) networks in toluene. Solid curves are the fit to Eq. 2

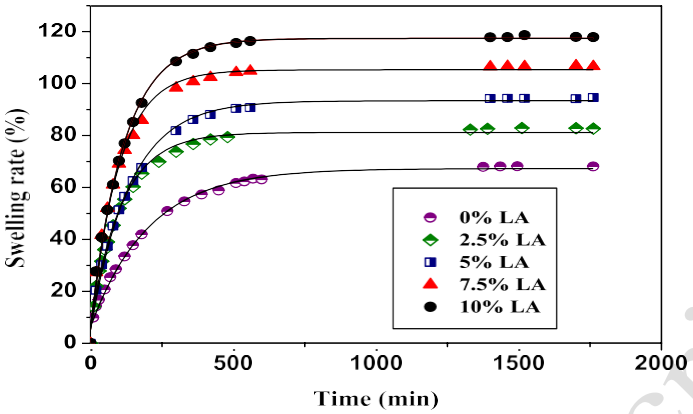

Fig. 14 Kinetics swelling of poly(PEA-*co*-LA/0.1%wt HDDA) networks in MIBK. Solid curves are the fit to Eq. 2

where *C′* represents the ratio of the co-monomer (wt% LA).

As the degree of lauryl acrylate (wt% LA) increases, the diffusion capacity of the solvent molecules inside the polymer network increases. This returns to two reasons, firstly, the geometric change of networks, i.e., a magnification at the mesh levels. Due secondly to the linear chemical structure of the new introduced monomer, therefore the interaction in the system, solvent/poly(PEA-co-LA), can be varied.

The variation behavior of the equilibrium degree of swelling as a function of the degree of the co-monomer (wt% LA) is illustrated in Fig. 16. Equations 23 and 24 express the linear relationship found

between the equilibrium swelling

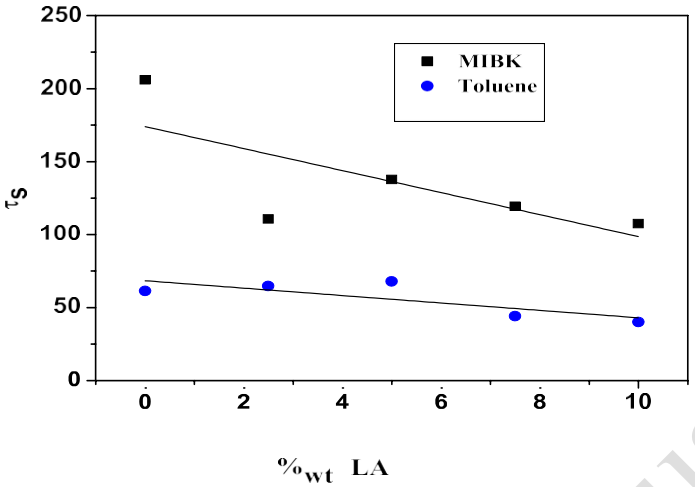

Fig. 15 Swelling time constant (τ_s) versus (%wt LA). Lines are guides to the eye

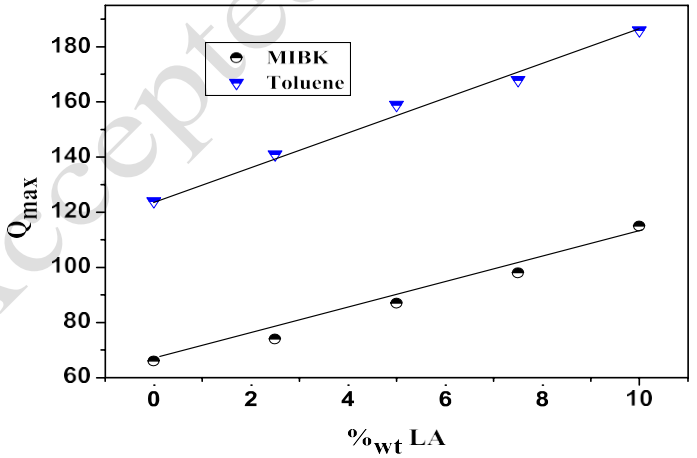

Fig. 16 Equilibrium degree of swelling (Q_{max}) versus (wt% LA). Lines are guides to the eye

and degree of the co-monomer (wt% LA) for both systems swollen in toluene and MIBK, respectively.

$$Q_{max} = 63.6 + 4.88\ C' \quad (23)$$

$$Q_{max} = 125 + 4.04\ C' \quad (24)$$

The swelling equilibrium increases proportionally with the degree of lauryl acrylate co-monomer (wt% LA). This is due to the internal mobility increases, which

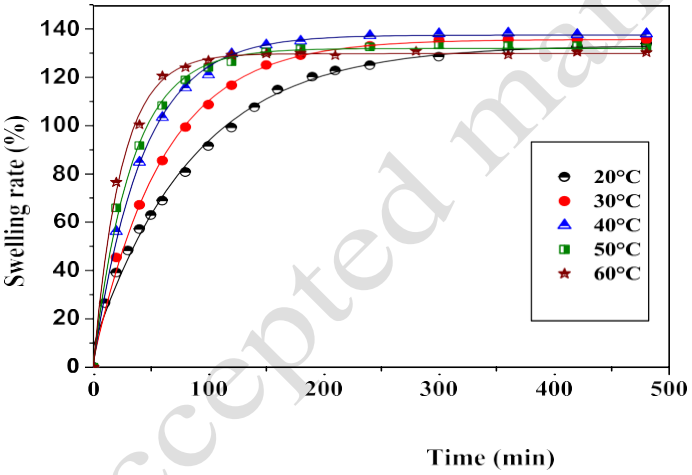

Fig. 17 Thermal effect on the kinetics swelling of poly(PEA/0.1wt% HDDA) networks in toluene. Solid curves are the fit to Eq. 2

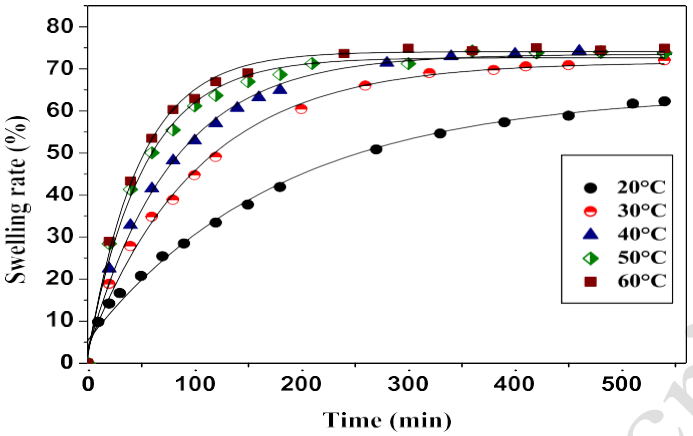

Fig. 18 Thermal effect on the kinetics swelling of poly(PEA/0.1wt% HDDA) networks in MIBK. Solid curves are the fit to Eq. 2

affect the elasticity and viscosity of the polymer chains; interestingly, these results were proved previously in glass transition examination, and a good correlation is noted between DSC and swelling results.

Temperature effect

Figures 17 and 18 show the influence of temperature on the swelling kinetics of the poly(PEA/0.1wt% HDDA) in toluene and MIBK, respectively. Note that the temperature slightly influences the Q_{max} in the case of MIBK; this influence is not observable in the case of toluene. However, this parameter has an influence on the rise of curves in both cases; at higher temperatures, the equilibrium is

reached earlier than that at room temperature and a best theoretical fits to the experimental data are noted.

The variation of the swelling time constant with the temperature is illustrated in Fig. 19. The behavior of the variation of the swelling time constant τ_s as a function of temperature for the two systems (poly(PEA/0.1wt% HDDA)/toluene and poly(PEA/0.1wt% HDDA)/MIBK) seems to follow the exponential law of Arrhenius, expressed on Eq. 25:

$$\tau_s = \tau_0 . \exp\left(-\frac{E_a}{RT}\right) \qquad (25)$$

where τ_0 is a given constant and E_a is the activation energy of the mobility chains, whose values are 30.45 kJ mol^{-1} and 48.33 kJ mol^{-1} for toluene and MIBK, respectively.

Determination of phase diagrams

Experimental phase diagrams are represented in the case of thermodynamic equilibrium for the flexible poly(PEA/0.1wt% HDDA) network swelled in toluene and MIBK. Each point of the curve corresponds to the swelling equilibrium values of the swelling kinetics curves.

Figure 20 illustrates the variations of the temperature as a function of

the mass fraction of the solvent defined by Eq. 8. All systems show a large region on the left-hand side of the figure, where a single phase appears at low solvent volume fractions. The biphasic region of the polymer network and isotropic solvent can be found on the right hand side of the diagram.

The phase diagram of the poly(PEA/0.1wt% HDDA) swollen in toluene is represented by a vertical line indicating independence with temperature. This is explained

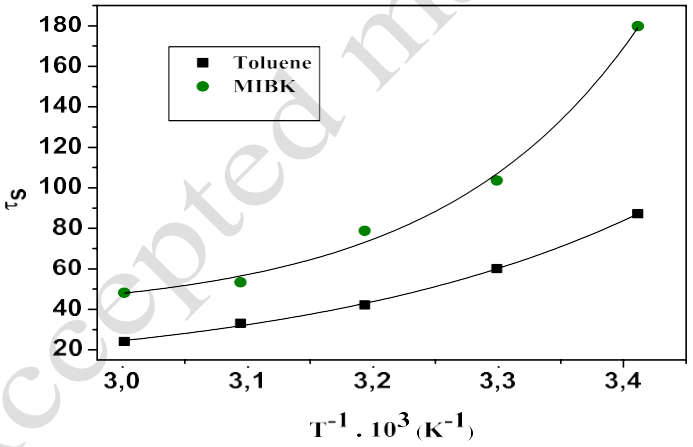

Fig. 19 Swelling time constant (τ_s) versus $1/T$

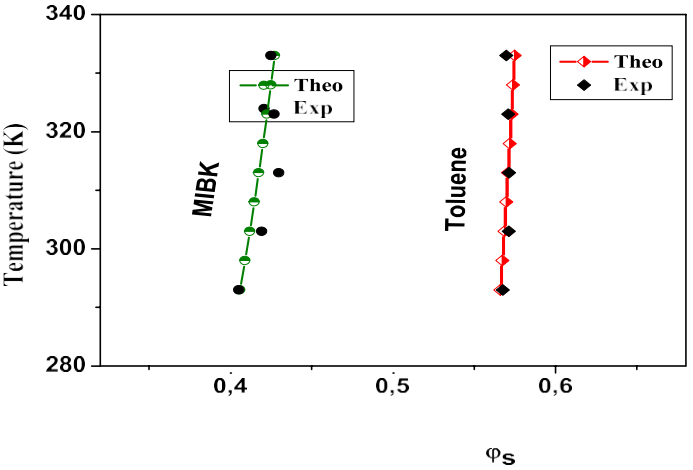

Fig. 20 Phase diagrams experimental and theoretical of poly(PEA)/0.1wt% HDDA/solvents

by the miscibility of solvents in the polymer network. In addition, it can be noted that the phase diagram of the poly(PEA/0.1wt% HDDA)-MIBK system is not linear; in fact, there is a slight temperature dependence corresponding to a low miscibility polymer/solvent. Using Eqs. 13 and 14, the theoretical phase diagrams were obtained and represented by solid-symbol lines. The phase diagrams calculated from the theoretical model show a good correlation with the experimental phase diagrams.

Calculation of the thermodynamic quantities, ΔH, ΔS and ΔG

Assuming that ΔH and ΔS remain constant during the temperature range studied (20–60 °C), in Fig. 21, the log K_s as a function of $1/T$ is

linear, and ΔH and ΔS are

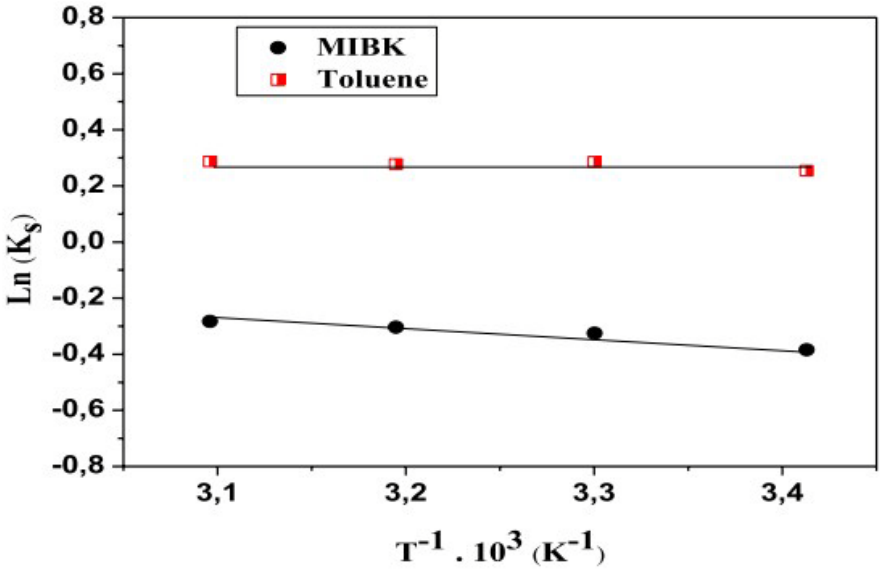

Fig. 21 van't Hoff plot of log (K_s) versus de 1/T. Lines are guides to the eye

obtained, respectively, from the intersection and the slope. These results are shown in Table 3.

The positive ΔH values obtained for both solvents suggest that the absorption, in this case, is dominated by the Henry model [29] with endothermic contributions. However, ΔS values are positive.

Table 3 Values of ΔH, ΔS and ΔG of the swelling process

Solvent	ΔH (kJ mol^{-1})	ΔS (J mol^{-1})	ΔG (kJ mol^{-1})
Toluene	0.32	6.2936	− 1.4
MIBK	5.93	13.06	2.36

The change in ΔG was obtained using expression 17; the standard Gibbs absorption energy ΔG is positive at room temperature for the poly(PEA)/MIBK system which was an indication of the non-spontaneity of the mixing solubility. In contrast, the negative value of ΔG of the poly(PEA)/toluene system indicates the feasibility and spontaneity of the swelling process.

Conclusions

A cross-linked poly(PEA) was elaborated by facile, cleanest method, the UV photopolymerization technique. Samples were studied by swelling and DSC characterization; the Voigt model was applied to analyze the swelling results.

Based on the differential enthalpy analysis, the increase in the cross-linking degree increases the glass transition temperature of poly(PEA), whereas the copolymerization by an aliphatic monomer decreases the

T_g temperature. This is due to the internal mobility of the system.

The degree of swelling of poly(PEA) is proportional to the degree of copolymerization by aliphatic lauryl acrylate monomer; this is explained by the exploitation of the Voigt viscoelastic model, and the model shows that the variation in swelling rate follows a power law related to the degree of cross-linking. The inclusion of a small amount of aliphatic lauryl acrylate monomer between the aromatic monomers of the main chains increases both the mobility and the viscosity of the chains; therefore, the degree of swelling is increased.

Analysis of the swelling rates shows that toluene is a good solvent compared to MIBK. Theoretically confirmed by the calculation of the solubility parameter using the model Hoftyzer and Van Krevelen HVK, the solubility of poly(PEA) in toluene and MIBK is, respectively, 2.69 and 8.06.

The thermal study shows that the temperature does not influence the power parameter Q_{max}, but it has an effect on the rise to reach the plateau at equilibrium swelling.

The temperature increases the chain's flexibility of the polymer network, which activates the movement of the solvents molecules; consequently, their diffusion in polymer networks was more quickly. The variation of τ_s as a function of temperature has an exponential form

that corresponds well to Arrhenius law.

The free Gibbs energy indicates that ΔG is positive at 20 °C for the poly(PEA)/MIBK system which is an indication of the non-spontaneity of the mixing solubility. The negative value of ΔG of the poly(PEA)/Toluene system indicates the feasibility and spontaneity of the swelling process.

Acknowledgements The authors gratefully acknowledge the support of the Algerian Ministry of Higher Education and Scientific Research MESRS and the French Ministry of Higher Education, Research and Innovation MESRI.

References

1. Abdelaty MSA (2018) Environmental functional photo-cross-linked hydrogel bilayer thin films from vanillin (part 2): temperature-responsive layer A, functional, temperature and pH layer B. Polym Bull 75:4837–4858. https://doi.org/10.1007/s00289-018-2297-y

2. Tally M, Atassi Y (2016) Synthesis and characterization of pH-sensitive superabsorbent hydro- gels based on sodium alginate-*g*-poly(acrylic acid-*co*-acrylamide) obtained via an anionic sur- factant micelle templating under microwave irradiation. Polym Bull 73:3183–3208. https://doi. org/10.1007/s00289-016-1649-8

3. Zhao W, Odelius K, Edlund U, Zhao C, Albertsson AC (2015) In situ synthesis of magnetic field-responsive hemicellulose hydrogels for drug delivery. J Biomacromol 16:2522–2528. https://doi.org/10.1021/acs.biomac.5b00801

4. Doi M, Matsumoto M, Hirose Y (1992) Deformation of ionic polymer gels by electric fields. Macromolecules 25:5504–5511. https://doi.org/10.1021/ma00046a058

5. Yang R (2018) Analytical methods for polymer characterization. CRC Press, Boca Raton

6. Ganji F, Vasheghani-farahani S (2010) Theoretical description of hydrogel swelling: a review. Iran Polym J 19:375–398

7. Mark JE (2007) Physical properties of polymers handbook. Springer, New York

8. Treloar LRG (2009) The physics of rubber elasticity. Clarendon Press, Oxford

9. Karimi AR, Rostaminejad B, Rahimi L, Khodadadi A, Khanmohammadi H, Shahriari A (2018) Chitosan hydrogels cross-linked with tris(2-(2-formylphenoxy) ethyl) amine: swelling and drug delivery. Int J Biol Macromol 118:1863–1870. https://doi.org/10.1016/j.ijbiomac.2018.07.037

10. Qamar SZ, Pervez T, Akhtar M (2016) Performance evaluation of water-swelling and oil-swelling elastomers. J Elastomer Plast 48:535–545

11. Kizil S, Sonmez HBJ (2017) Oil loving hydrophobic gels made from glycerol propoxylate: efficient and reusable sorbents for oil spill clean-up. J Environ Manag 23:330–339. https://doi.org/10.1016/j.jenvman.2017.02.016

12. Zhang C, Yang D, Zhang T, Qiu F, Dai Y, Xu J, Jing Z (2017) Synthesis of MnO_2/poly(*n*- butyl-acrylate-*co*-butyl methacrylate-*co*-methyl methacrylate) hybrid resins for efficient oils and organic solvents absorption. J Clean Prod 148:398–406. https://doi.org/10.1016/j.jclep ro.2017.02.009

13. Hoang AT, Le VV, Al-Tawaha ARMS, Nguyen DN, Noor MM, Pham VV (2018) An absorption capacity investigation of new absorbent based on polyurethane foams and rice straw for oil spill cleanup. J Petrol Sci Technol 136:361–370. https://doi.org/10.1080/10916466.2018.1425722

14. Flory PJ, Rehner J (1943) Statistical mechanics of cross-linked polymer networks II. Swelling. Chem Phys 11:521–526. https://doi.org/10.1063/1.1723792

15. Tanaka T (1978) Collapse of gels and the critical endpoint. Phys Rev Lett 40:820–823. https://doi. org/10.1103/PhysRevLett.40.820

16. Kowalski G, Kijowska K, Witczak M, Kuterasiński Ł, Łukasiewicz M (2019) Synthesis and effect of structure on swelling properties of hydrogels based on high methylated pectin and acrylic polymers. J Polymers 11:114–130. https://doi.org/10.3390/polym11010114

17. Ida S, Kawahara T, Kawabata H, Ishikawa T, Hirokawa Y (2018) Effect of monomer sequence along network chains on thermoresponsive properties of polymer gels. J Gels 4:22–34. https://doi. org/10.3390/gels4010022

18. Bendahma YH, Hamri S, Merad M, Bouchaour T, Maschke U (2018) Conformational modeling of the system pollutant/three-dimensional poly(2-hydroxyethyl methacrylate) (PHEMA) in aqueous medium: a new approach. J Polym Bull 76:1517–1530. https://doi.org/10.1007/s00289-018-2455-2

19. Omidian H, Hashemi SA, Sammes PG, Meldrum IG (1998) A model for the swelling of superab- sorbent polymers. J Polym 39:6697–6704. https://doi.org/10.1016/S0032-3861(98)00095-0

20. Pourjavadi A, Jahromi PE, Seidi F, Salimi H (2010) Synthesis and swelling behavior of acrylated- starch-*g*-poly(acrylic acid) and acrylated starch-*g*-poly(acrylamide) hydrogels. J Carbohydr Polym 79:933–940. https://doi.org/10.1016/j.carbpol.2009.10.021

21. Lejcuś K, Spitalniak M, Dabrowska J (2018) Swelling behavior of superabsorbent polymers for soil amendment under different loads. J Polym 10:271–283. https://doi.org/10.3390/polym10030271

22. Van Krevelen DW, TeNijenhuis K (2009) Properties of polymers: correlations with chemical structure, 4th edn. Elsevier, Amsterdam

23. Barton AFM (1991) CRC handbook of solubility parameters and other cohesion parameters, 2nd edn. CRC Press, Boca Raton

24. Small PA (1953) Some factors affecting the solubility of polymers. J Appl Chem 3:71–80.

https:// doi.org/10.1002/jctb.5010030205

25. Flory PJ, Rehner J (1943) Statistical mechanics of cross-linked polymer networks I. Rubber-like elasticity. J Chem Phys 11:512–520. https://doi.org/10.1063/1.1723791

26. Benmouna F, Maschke U, Coqueret X, Benmouna M (1999) Model phase diagrams of binary nematic mixtures. A comparative study between linear and crosslinked polymers. Macromol Theory Simul 8:479–491. https://doi.org/10.1002/(SICI)1521-3919(19990901)8:5%3c479:AID-MATS4 79%3e3.0.CO;2-9

27. Petrovic ZS, MacKnight WJ, Koningsveld R, Dusek K (1987) Swelling of model networks. Macromolecules 20:1088–1096. https://doi.org/10.1021/ma00171a036

28. Aithal US, Aminabhavi TM (1990) Diffusivity, permeability, and sorptivity of aliphatic alcohols through polyurethane membrane at 25, 44, and 60 °C. J Chem Eng 35:298–303. https://doi.org/10.1021/je00061a021

29. Bamgbose JT, Bamigbade A, Adewuyi S, Dare EO, Lasisi AA, Njah N (2012) Equilibrium swelling and kinetic studies of highly swollen chitosan film. J Chem Chem Eng 6:272–283. https://doi.org/10.17265/1934-7375/2012.03.012

Affiliations

Nouara Benmessaoud[1] Salah Hamri[1,2]· Tewfik Bouchaour[1]

Ulrich Maschke[3]

Nouara Benmessaoud nouarab87@gmail.com

Tewfik Bouchaour bouchaour@yahoo.fr

Ulrich Maschke ulrich.maschke@univ-lille1.fr

1 Laboratoire de Recherche sur les Macromolécules (LRM), Faculté des Sciences, Université, Abou Bekr Belkaid, BP119, 1300 Tlemcen, Algeria

2 Centre de Recherche Scientifique et Technique en Analyses Physico-chimiques, BP 384, Zone Industrielle Bou-Ismail, 42004 Tipaza, Algeria

3 Unité Matériaux et Transformation (UMET), UMR8207(CNRS), Université de Lille 1-Sciences et Technologies, Bâtiment C6, 59655 Villeneuve d'Ascq Cedex, France